

Study on the effects of processing parameters on the CVD alumina coating

Nasim Chenari, Mansour Soltanieh and Arash Yazdani*

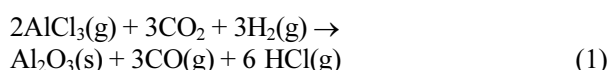
Centre of Excellence for High Strength Alloys Technology, School of Metallurgy and Materials Engineering, Iran University of Science and Technology, Tehran 16844, Iran

The CVD alumina coatings were deposited on carbide cutting tools using gas mixtures of H_2 , CO_2 and $AlCl_3$ at the temperatures between 960–1000 °C, one atmosphere pressure and for different gas flows of H_2 , CO_2 . The $AlCl_3$ gas is produced in a generator by passing the HCl gas through the mechanically worked aluminium granules. In a simulated laboratory set-up it was found that the reactivity of aluminium granules with HCl was increased drastically. Thickness measurements showed that by using worked granules, the alumina thickness for the same conditions increases from 0.75 to 3 μm . Moreover, it was found that with increasing the coating temperature and flow of gases, deposition rate was increased. Calculations showed that the process is far from the equilibrium condition. It was found that the reaction is kinetically mass transfer controlled in the boundary layer. The activation energy of the process was equal to 207.02 KJ/mol.

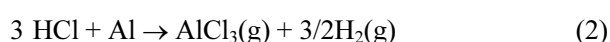
Key words: CVD, Aluminium granules, Mechanical working, Activation energy.

Introduction

Cemented carbide cutting tools are widely used in metal machining industry. The cutting tools have to withstand in sever condition of machining such as high temperature, high pressure, erosion and thermal shocks. Because of the high vertical forces, quick movement of the metallic chips on the surface of cutting tools and high temperatures, the cutting tools are eroded. Therefore, the surface of the cutting tools is coated with especial materials [1-3]. Multilayer Ti (C, N) and Al_2O_3 coatings are commonly used as protective coatings for cemented carbide cutting tools. Due to low thermal conductivity and high hardness, alumina is an excellent thermal barrier to prevent temperature increase substrate materials [4, 5]. Large variety of methods such as Conventional thermal chemical vapor deposition (CVD) [6, 7], plasma-enhanced CVD (PECVD) [8, 9] and laser chemical vapor deposition have been used for the deposition of alumina coating on cutting tools. The alumina is produced by the following reaction:



The $AlCl_3$ (g) is produced by the following reaction:



A variety of different characteristics of the alumina polymorphs could be achieved by varying the production parameters such as temperature, gas composition, gas velocity and finally by using doping elements like Ti, B, N and others to achieve complex doped Al_2O_3 [10].

Many researchers have investigated the effects of deposition temperature and feed gas composition [11], total pressure [12] and using different amounts of various doping compounds [10, 13] on the coating characteristics and growth kinetics. Accordingly, different activation energies have been reported [14]. One can see that some aspects of CVD alumina coating process are still left. For example, according to equation 1 the quality of aluminum granules has a great effect on the process efficiency and coating thickness. Consequently, in this research the effect of using mechanically worked aluminum granules, temperature and gas flow on the growth kinetics of alumina coating was studied. Besides, experimental data were compared to those obtained from FactsageTM 5.3 software.

Experimental Procedure

Al_2O_3 coatings were deposited on a TiCN base layer using cemented carbide substrates by CVD. An industrial-scale hot-wall CVD plant in Almaseh Saz Company of Iran was used. The temperature during Al_2O_3 deposition was between 960–1000 °C, the deposition pressure was 1 atm. The deposition time was kept constant at 3 hr. H_2 , CO_2 and $AlCl_3$ were used as feed gases. Three different flow rates for H_2 : 15, 18, 20 l/min and CO_2 : 1.2, 1.3 and 1.4 l/min were selected. $AlCl_3$ is generated by passing HCl gas through the

*Corresponding author:
Tel : +98-217-7240503
Fax: +98-217-7240500
E-mail: arash_yazdani@metaleng.iust.ac.ir

Al granules. The granules are disc-type shape, with about 10 mm in diameter and a thickness of about 4 mm. About 6 kg of Al granules are charged into a generator at 220 °C. In Fig. 1 a schematic diagram of the industrial set-up is shown. The nitrogen and hydrogen gases are used as the carrier gas and reduction gas, respectively.

To evaluate the effect of mechanical working on the

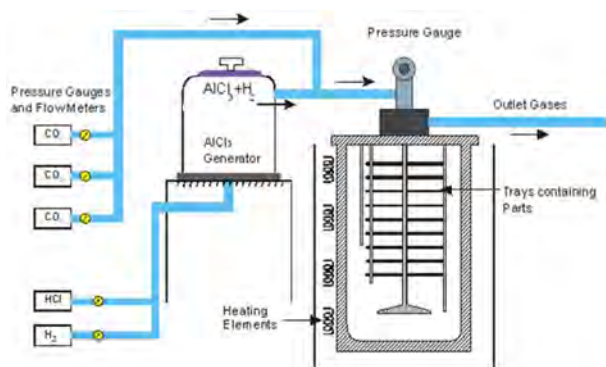


Fig. 1. Schematic diagram of Industrial set-up used for alumina CVD deposition.

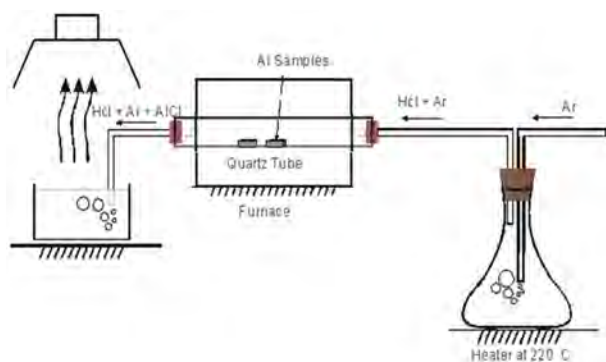


Fig. 2. Schematic diagram of simulated set-up used in this research for the production of AlCl_3 .

reactivity of aluminum granules, an electrolytic aluminum plate (99.99%) with 4 cm thickness was rolled with 0, 33.3, 60, 80 and 93.3 percents of reduction. The hardness of aluminum samples before and after rolling was measured. A simulated set-up was prepared, as Fig. 2. Three pieces of Al rolled samples were weighted and the surface areas of those were measured. Al samples were put into the quartz tube. The quartz tube was placed in a resistance furnace at temperatures between 220 to 240 °C. An argon gas with a flow rate of 0.45 to 0.50 l/min was blown into a one molar HCl acid. The argon and HCl gases were passed over the samples for 15, 30 and 60 min. The off-gas contained HCl, H_2 , AlCl_3 and Ar gases. The off-gas was finally passed through water to eliminate AlCl_3 and HCl gases. The samples' weights were measured after the experiments. To normalize the results, the percentage of weight losses per surface area was determined.

One sample of each rolling condition was heated for one hour at 200, 300 and 350 °C to determine the annealing temperature. If the annealing temperature of the aluminum samples was below 240 °C, the effect of cold working (rolling) could be eliminated. The hardness of samples after annealing even at 350 °C was not changed, so the annealing temperature of samples is above 350 °C.

Optical microscopy (Metallopan 021911, Germany) was employed to measure the coating thickness. In order to investigate whether the deposition process is an equilibrium one or not, FactsageTM 5.3 software was used.

Results and Discussion

Mechanically worked aluminum granules with different percentages of rolling (0, 33.3, 60, 80 and 93.3) were charged into the simulated set-up for the production of

Table 1. Specifications of Al granules before and after reaction with HCl gas.

Reaction time, Min	Percentage of reduction	Hardness, HB	Samples surface area, cm^2	Initial weight, g	Final weight, g	Weight loss percentage per surface area, $(\Delta W/W) \times 100/A$
15	0	34.1	4.28	1.2909	1.2878	0.056
	33.3	36.0	5.08	1.4604	1.4348	0.344
	60	39.5	4.46	1.5812	1.4542	0.612
	80	40.1	4.18	1.1557	1.1227	0.682
	93.3	41.0	2.42	0.4874	0.4705	0.694
30	0	34.1	5.16	1.7157	1.6093	1.201
	33.3	36.0	4.12	1.1593	0.9949	3.441
	60	39.5	5.56	1.6631	1.2493	4.460
	80	40.1	4.98	1.3451	1.1203	4.512
	93.3	41.0	3.85	0.7069	0.0409	17.296
60	0	34.1	4.10	1.0371	0.6226	10.109
	33.3	36.0	4.36	1.0352	0.5591	10.560
	60	39.5	3.60	1.1305	0.5746	13.660
	80	40.1	4.22	1.0335	0.4288	13.860
	93.3	41.0	2.72	0.9129	0.3199	23.879

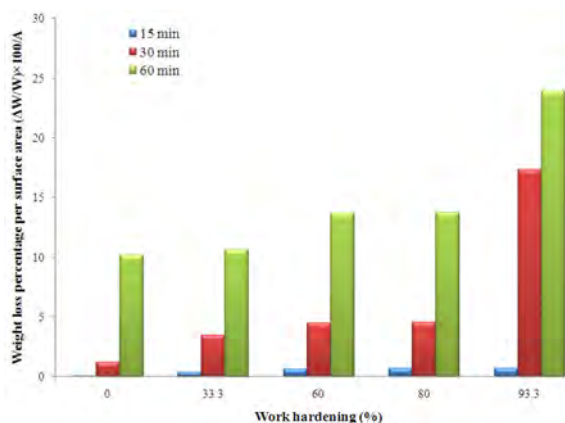


Fig. 3. The effect of the work hardening and exposing time on the percentage of the weight losses per surface areas of the Al granules.

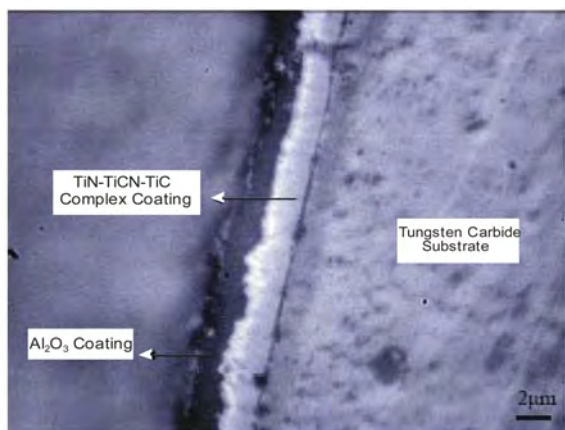


Fig. 4. Cross section of a carbide cutting tool coated with TiCN and then coated with CVD alumina for 5 hrs.

AlCl_3 gas. The experiment was conducted for 15, 30 and 60 min. Initial and final weight and surface area of granules were measured. Term “weights losses percentage per surface area” was defined as an indication for the reactivity of work hardened granules. Table 1 shows the results of measurements and calculations.

In Fig. 3, the effect of work hardening on the corrosion of Al samples is shown. Cold working increases the density of grain boundaries and structural defects such as dislocation density. It is clear that structures with these features have lower corrosion resistance. As a result, samples with higher percentage of cold working and longer exposure time are more corroded compared to other ones. For example it can be seen, sample with 93.3% work hardening and exposure time of 60 min reacts drastically with the HCl gas and shows 23.9% weight losses per surface while sample without work hardening shows only 0.05% weight losses per surface after 15 min reacting time. It is seen that using work hardened aluminum together with relatively longer exposure time, increases the efficiency of AlCl_3 production more than 450 times.

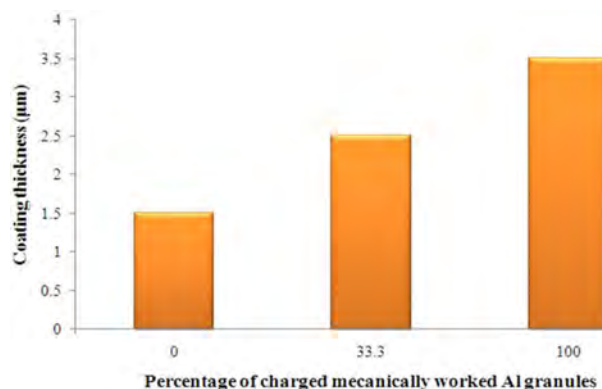


Fig. 5. The effect of the percentage of worked granules on the alumina thickness (CO_2 flow rate = 1.3 l/min, H_2 flow rate = 15 l/min, $T = 965^\circ\text{C}$).

In the second phase of this research, industrial Al granules were rolled about 80% reduction in thickness. The Al granules hardness was increased from 18 HB to 40.1 HB. The Al granules capacity of the generator for AlCl_3 production is 6 kg. In three different sets of experiments 0, 33 and 100 percent of generator capacity was filled by worked Al granules. The H_2 and HCl gases were passed through the Al granules in the generator for about 5 hrs. The off gas was injected in the furnace. About 3000 pieces of cutting tools were placed in the furnace. The furnace temperature was set between 960 and 1000 $^\circ\text{C}$. The coating procedure was the same in all experiments. After the coating cycle, the samples were sectioned by water-cooled cutter. The thicknesses of the coated samples were determined by optical microscope. In Fig. 4a typical SEM image of cross section of carbide cutting tool coated with alumina is shown. As can be seen in Fig. 4, two different layers of TiCN and Al_2O_3 are distinguished. Fig. 5 shows the effect of the percentage of worked granules on the alumina coating thickness.

The alumina thickness for the same procedure is increased from about 1.5 to 3.5 μm . It is just because of the using work hardened aluminum granules. According to the equation 2, reaction between HCl and Al granules is close to completion. Therefore, more AlCl_3 gas is produced and less unreacted HCl gas is left in the furnace atmosphere. The Gibbs' free energy of the equation 1 is as the following:

$$\Delta G = \Delta G^\circ + R \times T \times L \frac{(P_{\text{HCl}})^6 \times (P_{\text{CO}})^3}{(P_{\text{AlCl}_3})^2 \times (P_{\text{CO}_2})^3 \times (P_{\text{H}_2})^3} \quad (3)$$

Since there is less HCl and more AlCl_3 available, therefore, the Gibbs' free energy is more negative. Consequently, based on the Le Chatelier's principles the reaction 2 has to be moved from left to right to compensate this change in system. Finally, the rate of alumina deposition will be increased. It is in agreement with the observations.

Table 2. Summary of deposition rate and specifications for CVD Al₂O₃.

Technique	Precursors	T (K)	Deposition rate (μm/h)	Ref.
Thermal CVD	AlCl ₃ -CO ₂ -H ₂	1238	0.2-0.6 ^c	This work
	AlCl ₃ -CO ₂ -H ₂ -H ₂ S	1073	0.4	[14, 15]
	AlCl ₃ -CO ₂ -H ₂ -H ₂ S	1073-1273	0.1-0.7	
	AlCl ₃ -CO ₂ -H ₂	1273-1473	1-20	[16]
	AlCl ₃ -CO ₂ -H ₂ -H ₂ S	1273	0.9	[7]
Combustion CVD	Al(acac) ₃	1323-1398	3-6	[17]
MOCVD ^a	Al(acac) ₃	523-873	0.6	[18]
		1070	0.25	[19]
		873-1273	2.7-3.9	[20]
		773-1273	0.8-1.5	[21]
	Aluminium Tri-Isopr opoxide	1273-1373	2-6	[22]
LCVD ^b	Tri Methyl Aluminium	523	0.5	[23]
	Al(acac) ₃	970-1100	570	[24]
		1060-1120	370	
		1100-1280	250	

^aMetal Organic CVD, ^bLaser CVD, ^cWhen mechanically worked aluminium granules are used for AlCl₃ production.

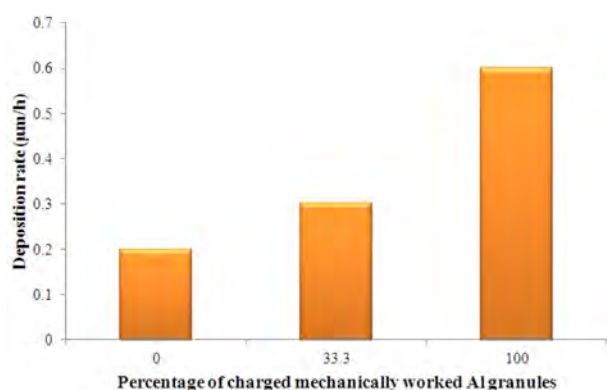


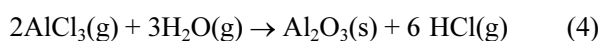
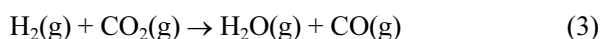
Fig. 6. The effect of the percentage of worked granules on the coating deposition rate (CO₂ flow rate = 1.3 l/min, H₂ flow rate = 15 l/min, T = 965 °C).

It can be seen in Fig. 6 that by increasing the amount of worked aluminium granules, deposition rates increase as well.

A summary of deposition rates of CVD alumina coating together with some process specifications have been tabulated in Table 2.

In comparison to other parameters, the percentage of mechanically worked Al granules has a distinct effect on the deposition rate.

It is well known that CVD alumina deposition (Eq. 1) involves two different types of reactions: homogenous gas-phase and heterogeneous surface reactions. The homogenous reaction is kinetically limited by the water-gas shift (Eq. 3). According to Eq. 4, H₂O which is produced in situ in the reactor chamber reacts with AlCl₃ and forms Al₂O₃ coating [14].

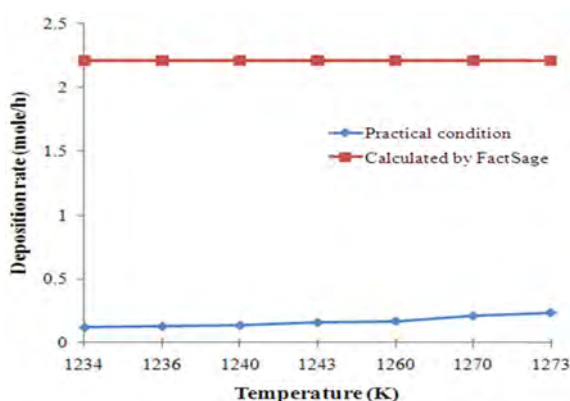


Surface reaction between aluminum halide and an oxygen donor is another contribution of Al₂O₃ growth. The relative contribution of these reactions to the growth of Al₂O₃ keenly depends on the free volume adjacent to the surface to be coated [25-27]. In order to make this parameter more tangible, the V/A ratio, free volume around the substrate, has been defined. This approximation gives: $V = a \times b \times l$, $A = 2 \times b \times l$. So $V/A = a/2$ is obtained, where “a” is the separating distance between two plates having the infinite area of $b \times l$ [14]. Up to here it was found that reactor geometry (e.g. volume-to-surface ratio) may strongly affect the relative contribution of homogenous and heterogeneous surface reactions which will result in different deposition characteristics of CVD alumina coatings. For example it is generally assumed that at higher volume-to-surface ratios the homogenous reaction where the water gas shift reaction is rate controlling becomes important. Or by increasing the process pressure, deposition rate improves which is related to increasing the contribution of homogenous gas-phase reaction [26, 27]. It is believed that the deposition rate and gas pressure are exponentially [26, 28] and linearly [14] related to each other. Generally, total pressure and V/A ratio are known as key factors affecting the growth rate of Al₂O₃. It should be noticed that doping process gases with some gases such as H₂S may enhance the deposition rate as well. In industrial practices, sometimes H₂S is used to promote the deposition rate. Moreover, H₂S doping increases the surface controlled contribution of Al₂O₃ which consequently enhances the coating uniformity [14].

It can be concluded that several parameters such as V/A ratio, total pressure, type and amount of doping compound and temperature affect the deposition rate.

Table 3. The effect of temperature on the deposition rate of alumina coating.

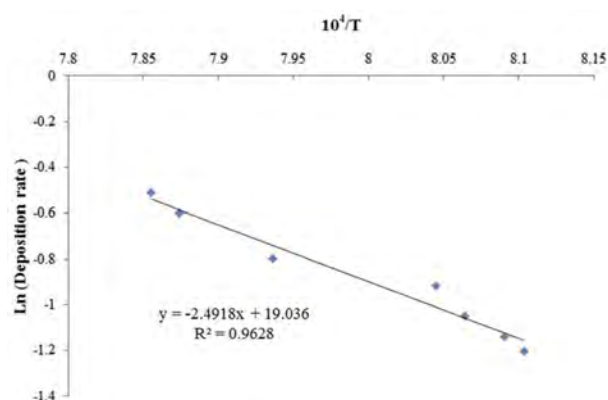
T(K)	Deposition rate, ($\mu\text{m/h}$)	Surface area of samples, cm^2	Coating volume, cm^3	Deposition rate, (mole/h)
1234	0.30	17424	3.055	0.119
1236	0.32	17752	3.269	0.127
1240	0.35	13948	3.443	0.134
1243	0.40	16204	4.025	0.157
1260	0.45	10800	4.258	0.167
1270	0.55	12726	5.343	0.209
1273	0.60	15428	5.991	0.234

**Fig. 7.** The effect of the temperature on the coating deposition rate (CO_2 flow rate = 1.3 l/min, H_2 flow rate = 15 l/min, charged worked granules = 33.3%).

Therefore, comparison between the results of different researches seems to be difficult. In one case, since an industrial reactor was used in this research, three thousands of inserts were coated in one run. Because of economic issues inserts were arranged very compactly in the reactor. It is clear that in this case the separating distance between inserts decreases which will result in lower V/A ratio and consequently lower deposition rate.

According to Fig. 6, it can be seen that by replacing all granules with worked one, deposition rate increases around three times.

In the next step for more detail study, 33% of the AlCl_3 generator of the coating chamber was charged with the Al work hardened granules. The surface area of the inner parts of the furnace was 84417 cm^2 . In each set of the coating process, the surface area of all of the samples was measured as well. The total deposited moles of alumina were determined. For example in one set of experiments at 961°C , the surface area of all of the cutting tools was 17424 cm^2 . The coating thickness of the parts was $3 \mu\text{m}$. The volume of the deposited alumina was calculated as 3.055 cm^3 . Therefore, the total number of moles of deposited alumina per hour is 0.119 moles. In table 3 and Fig. 7 the effect of temperature on the deposition rate of coating, in the form of the number of alumina mole per hour (moles/hour), is shown. As can be seen

**Fig. 8.** Variation of logarithm of deposition rate versus the reciprocal of absolute temperature.

in Fig. 7, by increasing the temperature from 1234 to 1273 K, deposition rate increases from 0.119 to 0.234 moles per hour, respectively. In fact, the deposition rate is increased about two times. This indicates that the deposition of the alumina is thermally activated reaction which is in agreement with the results of other researchers [10, 12].

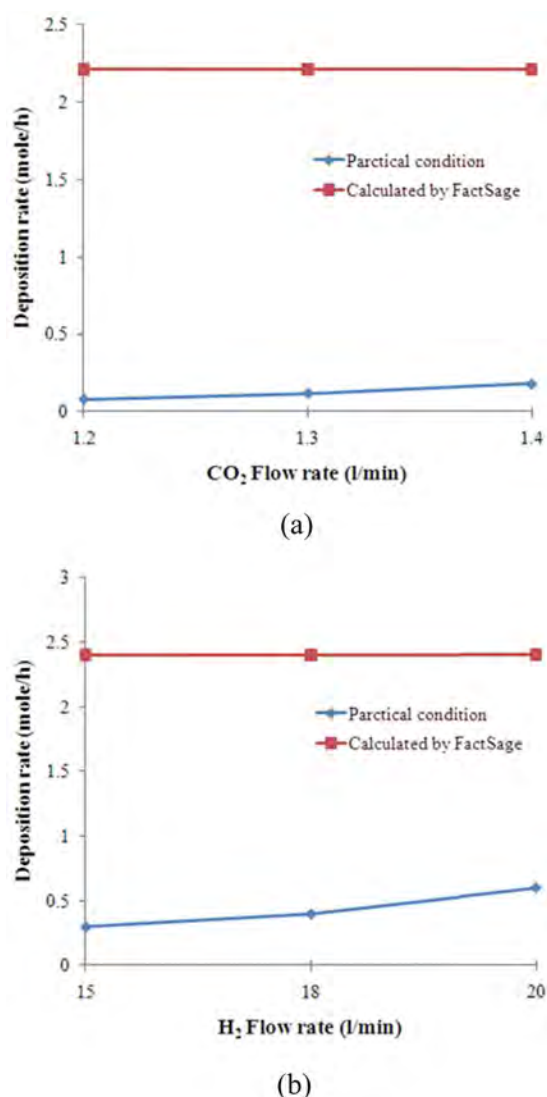
The FactSage software was used to determine the total number of moles of deposited alumina per hour. In Fig. 7 the results of the calculations of the software is shown as well. As can be seen from Fig. 7, the temperature changes do not have a dominant effect on the deposition rate. The real condition and the modeling calculation are quite different. It means that practical conditions are far from equilibrium ones. The Gibbs' free energy of the reaction between 1234 and 1273 K is around -332 kJ [29]. It means that there is a high tendency for the completion of reaction and consequently the formation of alumina coating. Since the amount of H_2 and CO_2 gas is much greater than equilibrium amount, the amount of AlCl_3 gas will determine the amount of deposited alumina coating. Therefore, if equilibrium condition rules during the whole coating process, the FactSage software gives a constant amount of deposited alumina coating in all process temperatures. Hence, the deposition rate would be constant and equals to 2.21 mole/hr. It is also seen that with increasing the temperature, the deposition rate increases and become a little closer to equilibrium condition but there is still far distance to reach.

In Fig. 8 the logarithm of deposition rate is drawn versus the reciprocal of absolute temperature. The slope of the curve at any temperature represents the activation energy of the reaction. A line with the equation: $\text{Ln}(\text{rate}) = -2.4918 \times (10000/T) + 19.036$ is fitted to the data in Fig. 8.

The slope of the line is -2.4918, which is equal to the $(-Q/R)$. Therefore, the activation energy for this process is equal to 207.02 kJ/mol. Since the mass transport condition is characterized with lower activation energy (100-300 kJ/mol), it is clear that deposition process

Table 4. Literature data on activation energies reported for Al_2O_3 .

Reaction	Doping	T (K)	P (mbar)	Activation energy (kJ/mol)	Reference
Al_2O_3 deposition	–	1233–1273	1013	207.02	This work
	$\text{H}_2\text{S} = 1\%$	1073–1273	50	–82	[14]
	–	1073–1273	50	–175	[14]
	–	1073–1273	300	–111	[14]
	$\text{H}_2\text{S} = 0.2\%$	1073–1273	300	–81	[14]
	–	1003–1188	1013	–95.5	[30]
	–	1173–1473	810	–64.9	[31]
	–	1173–1473	61	–131	[31]
	–	673–1273	1013	–237.4	[32]
	–	1273–1423	67	–150.7	[33]
	–	1273–1423	133	–146.5	[33]
Water gas reaction	–	1173–1323	1013	–326.6	[34]
	–	1148–1323	1013	–238.6	[35]

**Fig. 9.** Effect of gas flow rate (a) CO_2 and (b) H_2 on deposition rate at practical and simulated conditions ($T = 965^\circ\text{C}$, charged worked granules = 33.3%); (a) H_2 flow rate of 15 l/min, (b) CO_2 flow rate of 1.3 l/min.

in this study is mass transport controlled. A review of the reported activation energies is presented in Table 4.

It is seen that there are large differences between activation energy values. Most probably using different deposition conditions (for example V/A ratio) and widely differing experimental conditions are the main reasons for the span in reported activation energies.

Finally, the effect of H_2 and CO_2 flow rates on the deposition rate at simulated and practical conditions was studied (Fig. 9(a) and 9(b)).

According to Fig. 9, with increasing gas flow (either CO_2 or H_2), deposition rate increases in practical condition while in simulated one, FactSage calculation shows that deposition rate has a constant value of 2.21 and 2.4 mole/h for all CO_2 and H_2 flow rates, respectively.

As it was mentioned previously, deposition process in this study is controlled by mass transportation in boundary layer. Most probably, increasing gas flow (either CO_2 or H_2) leads to greater concentration gradients of reactants gases in boundary layer. Consequently, driving force for reactants diffusion through boundary layer increases which results in higher deposition rate.

Again, calculated results proved that coating process in this study is far from equilibrium conditions. This distance can be reduced by increasing flow rates of entering gasses.

Conclusions

Mechanical working on the aluminum granules had a great effect on the reactivity of granules with the HCl. The rate of AlCl_3 production was increased drastically. With increasing the rate of AlCl_3 production, the rate of alumina deposition on the carbide cutting tools was increased. Since the alumina production by the CVD is a thermally activated process, with increasing the temperature, the deposition rate is increased. Because

of the kinetic barriers, the process is far from the equilibrium conditions. The activation energy for the process was found to be equal to 207.02 kJ/mol. According to the calculations, it was found that the mass transfer in the boundary layer close to the substrate is controlling step.

Acknowledgments

The authors are thankful of the cooperation of Almase Saz Company of Iran to let us use their facilities, especially Dr. Mosavi and Mr. Rahimi.

References

1. A. Riedl, N. Schalk, C. Czettl, B. Sartory, C. Mitterer, *Wear* 289 (2012) 9-16.
2. H.K. Pulker, *Wear and Corrosion Resistant Coatings by CVD and PVD*, Ellis Horwood Limited Publication, United Kingdom (1989).
3. H.K. Tönshoff, A. Mohlfeld, *International Journal of Machine Tools and Manufacture* 38 (1998) 469-476.
4. H. Holleck, V. Schier, *Surf. Coat. Technol.* 76-77 (1995) 328-336.
5. K. Holmberg, H. Ronkainen, A. Matthews, *Ceram. Int.* 26 (2000) 787-795.
6. P. Hansson, M. Halvarsson, S. Vuorinen, *Surf. Coat. Technol.* 76-77 (1995) 256-264.
7. S. Ruppi, *Int. J. Refract. Met. Hard Mater.* 23 (2005) 306-316.
8. H. Wang, C. Lin, M. Hon, *Thin Solid Films* 310 (1997) 260-264.
9. M. Fink, J. Laimer, H. Störi, C. Mitterer, *Surf. Coat. Technol.* 200 (2005) 360-363.
10. M. Kathrein, W. Schintlmeister, W. Wallgram, U. Schleinkofer, *Surf. Coat. Technol.* 163-164 (2003) 181-188.
11. M. Pulver, W. Nemetz, G. Wahl, *Surf. Coat. Technol.* 125 (2000) 400-406.
12. R. Colmet, R. Naslain, *Wear* 80 (1982) 221-231.
13. D. Hochauer, C. Mitterer, M. Penoy, S. Puchner, C. Michotte, H.P. Martinz, H. Hutte, M. Kathrein, *Surf. Coat. Technol.* 206 (2012) 4771-4777.
14. S. Ruppi, A. Larsson, *Thin Solid Films* 388 (2001) 50-61.
15. A. Larsson, S. Ruppi, *Int. J. Refract. Met. Hard Mater.* 19 (2001) 515-522.
16. C. Park, J. Kim, J.S. Chun, *J. Vac. Sci. Technol A* 1 (1983) 1824.
17. V. Siva Kumar G. Kelekanjeri, W. Carter, J. Hampikian, *Thin Solid Films* 515 (2006) 1905-1911.
18. T. Maruyama, S. Arai, *Appl. Phys. Lett.* 60 (1992) 322-323.
19. S. Blittersdorf, N. Bahlawane, K. Kohse-Hoinghaus, B. Atakan, J. Muller, *Chem. Vap. Deposition* 9 (2003) 194-198.
20. A. Devi, S. Shivashankar, A. Samuelson, *J. Phys. IV France* 12 (2002) Pr4-139-146.
21. C. P. itsch, D. Viehhaus, U. Bergmann, B. Atakan, *Thin Solid Films* 515 (2007) 3653-3660.
22. R.H. Niska, A.P. Constant, T. Witt, O.J. Gregory, *J. Vac. Sci. Technol A* 18 (2000) 1653-1658.
23. M. Minakata, Y. Furuka wa, *J. Electro. Mater.* 15 (1986) 159-164.
24. H. Kadokura, A. Ito, T. Kimura, T. Goto, *Surf. Coat. Technol.* 204 (2010) 2302-2306.
25. C. Chateld, J.N. Lindstrom, M.E. Sjostrand, *J. Phys. C* 5 (1989) 1607-1611.
26. H. Schachner, J.N. Lindstrom, in: H.E. Hintermann Ed., *Proceedings of the 3rd European Conference on Chemical Vapour Deposition*, Neuchatel, Switzerland, April. 18 (1980) pp. 208.
27. J.N. Lindstrom, K.G. Stjenberg, in: J.O. Carlsson, J. Lindstrom (Eds.), *Proceedings of the 5th European Conference on Chemical Vapour Deposition*, Uppsala, Sweden, June. 17-20 (1985) pp. 169.
28. R. Funk, H. Schachner, C. Triquet, M. Kornmann, B. Lux, *J. Electrochem. Soc.* 123 (1976) 278-285.
29. A. Raine, *HSC Chemistry 1.10*, Outokumpo, Research OY, Pori, Finland (1993).
30. V.J. Silvestri, C.M. Osburn, D.W. Ormond, *J. Electrochem. Soc.* 125 (1978) 902-907.
31. R. Colmet, R. Naslain, P. Hagenmuller, C. Bernard, *J. Electrochem. Soc.* 129 (1982) 1367-1372.
32. K. Iida, T. Tsujide, *J. Appl. Phys.* 11 (1972) 840-849.
33. C.H. Park, J.G. Kim, J.S. Chun, in: J. Bloem, G. Verspui, L.R. Wolf Eds., *Proceedings of the 4th European Conference on Chemical Vapour Deposition*, Eindhoven, The Netherlands, May 31-June. 2 (1983) 401.
34. G.L. Tingey, *J. Phys. Chem.* 70 (1966) 1406-1412.
35. W.M. Graven, F.J. Long, *J. Am. Ceram. Soc.* 76 (1954) 2602-2607.